Relations between microbarograph and strain data

G. Mentes, I. Eper-Pápai

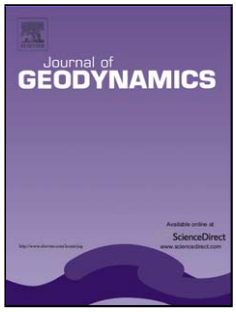

Title: Relations between microbarograph and strain data

Authors: G. Mentes, I. Eper-Pápai

PII: S0264-3707(09)00072-6
DOI: doi:10.1016/j.jog.2009.09.005
Reference: GEOD 899

To appear in: *Journal of Geodynamics*

Please cite this article as: Mentes, G., Eper-Pápai, I., Relations between microbarograph and strain data, *Journal of Geodynamics* (2008), doi:10.1016/j.jog.2009.09.005

Relations between microbarograph and strain data

G. Mentes*, I. Eper-Pápai

Geodetic and Geophysical Research Institute of the Hungarian Academy of Sciences;

Csatkai Endre u. 6-8., H-9400 Sopron, Hungary.

*Fax: +36-99-508-355

E-mail: mentes@ggki.hu

Abstract

The relationship between barometric and strain data related to seasonal characteristics within a year was studied on the basis of parallel records from a quartz tube extensometer and a microbarograph at the Geodynamical Observatory in Sopronbánfalva, Hungary. Both strain and barometric data series were combined into groups according to the three 'Lloyd' seasons and they were subjected to spectrum, tidal, regression and coherence analysis. All of the analysis methods establish long periods, with seasonally varying relations between atmospheric pressure and linear deformation measurements in the tidal frequency band. We found that the separate seasonal barometric correction of the strain data did not bring a notable improvement in the diurnal band, while in the semidiurnal band the improvement was about 10% better than correcting the whole year's data in a single step.

Keywords: Atmospheric pressure; Barometric correction; Coherence analysis; Strain; Tidal analysis

1. Introduction

Atmospheric loading is one of the major factors that effects extensometric measurements by loading and deforming the Earth's surface. Barometric pressure variations have a complex influence on this kind of measurement, which means that the changes of atmospheric pressure on the whole Earth contribute to local deformations at any point on the Earth's surface. The pressure changes cause a direct deformation of the Earth's solid crust; they also have an

indirect effect by changing the ocean loading. In addition atmospheric pressure variations take place in a wide timescale from seconds to years. Most papers deal with the effect of atmospheric pressure variations on gravimetric measurements, and therefore most authors investigate only the radial displacement of the Earth's crust (e.g. Sun, 1995; Kroner and Jentzsch, 1999; Boy et al., 2006). The effect of barometric pressure variations on extensometric measurements was less intensively studied, than the effects on gravimetric measurements. However the high sensitivity (better than 10^{-10} strain) of the extensometers makes it possible to use them for investigation of the Earth's interior. The barometric pressure induced "noise" may limit the extraction of very small signals of interest, e.g. long periodic tides, resonant elastic deformations of the Earth's crust, etc. Farrel (1972) computed deformation caused by surface load. Rabbel and Zschau (1985) investigated the deformations and gravity changes on the Earth's surface due to regional and global atmospheric pressure variations in the case of a spherical radially stratified Earth. It was found that the principal horizontal strains may have amplitudes up to 10^{-8} and $\pm 1.5 \cdot 10^{-9}$ for seasonal changes in the atmospheric pressure distribution. Van Dam and Wahr (1987) calculated the time dependent effects of global atmospheric pressures on surface point positioning measurements and on gravity observations. They found that the displacements and gravity fluctuations were somewhat smaller during summer than winter months. Probably this is why the existing barometric pressure reduction methods can only be used with a limited accuracy for correction of strain data. Another problem is that the removal or reduction of barometric disturbing signals from strain data series is much more difficult than with gravimetric measurements, since the barometrically induced strain also depends on the properties of the bedrock and on the topography in the vicinity of the observatory. This was investigated by comparing the atmospheric pressure effects on a surface and a deep station by Mentes and Eper-Pápai (2006). In the last decade some papers studied the attributes of disturbed strain

signals due to atmospheric pressure variations (e.g. Onoue and Takemoto, 1998). Among others, Kroner et al. (2005) and Steffen et al. (2005) investigated the physical transfer mechanism between the barometric pressure and strain changes by finite element modelling. At the Geodetic and Geophysical Research Institute (GGRI) of the Hungarian Academy of Sciences, some methods for removal of the barometric pressure variations from strain signals were also studied (Mentes, 2000; Eper-Pápai and Mentes, 2002). Since the regression method, – together with other methods (see also Kroner and Jentzsch, 1999) – was not effective enough to eliminate the atmospheric pressure effect from strain measurements, the aim of the present research is to study the seasonal properties of the effects of atmospheric pressure variations on strain measurements using extensometric and local atmospheric pressure records. In this paper the seasonal features of the barometric pressure, and relationships between air pressure and strain data were investigated by spectrum, tidal, regression and coherence analysis.

2. Observations and data pre-processing

The Sopronbánfalva (a suburb of Sopron) Geodynamical Observatory in Hungary is located on the Hungarian Austrian border in the eastern foreland of the Alps. Its coordinates are: latitude 47° 40’ 55’’ N; longitude 16° 33’ 32’’ E; height is 220 m a.s.l. The observatory is an artificial gallery driven into gneiss. The depth of the gallery is about 60 m (see Fig. 8). A much more detailed description of the observatory is given by Mentes (2005, 2008). In 1991 a 22 m long quartz tube extensometer with an azimuth of 116° was installed in the gallery about 30 m from the entrance. The displacement of the free end of the extensometer is measured by a differential capacitive transducer. The instrument is calibrated daily by a built-in magnetostrictive actuator (Mentes, 1991). In 1997 a highly sensitive (0.0024 hPa/mV) microbarograph was developed at the GGRI for studying atmospheric tides (Mentes, 2004). This instrument is installed separately from the extensometer in a room about 10 m from the

entrance and 20 m from the extensometer. In addition to strain and atmospheric pressure measurements, the inside and outdoor temperatures were also recorded. In the observatory the yearly and daily temperature variations are less than 0.5 °C and 0.05 °C, respectively. We did not find any correlation (correlation coefficient was 0.03) between the microbarograph, the strainmeter and the inside temperature data, so the direct effect of temperature on the instruments can be disregarded. In the middle of 2001, a high resolution 24 bits digital voltmeter was installed for digitizing extensometric, barometric and temperature data. For the sake of the uniform data series, we used only the data recorded between 2002 and 2006 in our investigations. They were collected with a sampling rate of one sample/minute and were filtered by the equipment's built-in anti-aliasing filter. To get one value per hour the data series were resampled by the decimate routine of the ETERNA 3.30 tidal analysis program (Wenzel, 1996). Data series were also filtered by a high pass filter, with a cut-off frequency of 0.8 cycles/day, before processing. For the strain analysis in the diurnal and semidiurnal tidal bands, K1 (P1K1 group) and S2 waves were chosen because the K1 lunisolar diurnal wave has about the same magnitude (58.4 percent of the magnitude of M2) as the S2 principal solar wave (46.6 percent of the magnitude of M2). According to K1 and S2 waves, the atmospheric tidal waves S1 and S2 were chosen for the barometric pressure analysis.

3. Investigation of the seasonal relationship between barometric pressure and strain data

3.1. Barometric pressure variation

We calculated the monthly averages and standard deviations of the hourly atmospheric pressure data in each year to study how the magnitude of the atmospheric pressure changes depends on the seasons. To present the variation of the barometric pressure in a simple way, the average of the standard deviations was calculated for each month of 2002-2006. These averages and their standard deviations are presented in Fig. 1. It can be clearly seen that the

barometric pressure variations (average line) and their standard deviations (SD line) are higher from October to April than from May to September.

3.2. Spectrum analysis

We determined Fourier amplitudes in the frequency range of K1 (P1K1) and S2 strain and S1 and S2 barometric waves in each month of the period we investigated to inspect the yearly behaviour of the tidal waves regarding both strain and air pressure measurements. Figure 2 represents one typical amplitude spectrum for both strain and pressure data. The spectral amplitudes were determined with an accuracy of about 0.25 nstr for deformation, and about 0.013 hPa for pressure data. Since only records of single months were subjected to spectrum analysis, those tidal waves which are close to each other in frequency (P1 and K1) cannot be separated and an annual periodic amplitude variation results. The theoretical strain tides for the same geographical location were calculated and monthly spectral amplitudes were determined and applied for correction of the amplitudes from the strain data. A simple subtraction was made between the measured and the theoretical amplitudes. This diminished the temporal tidal amplitude variations. Figure 3 presents the results of spectrum analysis obtained for the year 2006. Calculations in other years show similar a tendency. In Fig. 3 the measured and theoretical data amplitude differences (meas.-theor.), the barometrically corrected measured and theoretical data amplitude differences (correct.-theor.) and amplitudes from the measured pressure data (barog.) are delineated for both the diurnal and semidiurnal frequency bands. The barometric correction was completed by means of the regression method separately in each year in the investigated period. On the basis of the results obtained for 2002-2006, we found that in the semidiurnal band the amplitude difference changes are smaller than in the diurnal band, as shown in our example in Fig. 3. We ascertain from these results that in the diurnal band, the correction of the barometric effect did not cause a marked decrease of differences between corrected and theoretical amplitudes. Barometric correction

of deformation data seems to work moderately in the semidiurnal band where we observed a somewhat evened amplitude course of the corrected data.

3.3. Tidal analysis

Through the following calculations we examined tidal parameter relationships on the basis of the seasonal characteristics of air pressure, due to the global pressure system variations. Both extensometric and barometric data were classified into seasonal groups, according to the three 'Lloyd' seasons denoted by "D", "E" and "J" months for tidal and regression analysis (Chapman and Lindzen, 1970). D months are: November, December, January and February (centred on the winter solstice); J months are: May, June, July and August (centred on the summer solstice) and E months are: March, April, September and October (centred on the equinoxes). This grouping takes the similar weather conditions and barometric pressures into consideration for the investigations. Tidal parameters were calculated by means of the ETERNA 3.30 tidal analysis program (Wenzel, 1996) using the Wahr-Dehant Earth model (Wahr, 1981; Dehant, 1987). Calibrated atmospheric pressure data was subjected to the analysis as a gravitational component, giving adjusted amplitudes in the original physical unit. In the tidal model, amplitude lines around only S1 and S2 waves were applied. Yearly data series (2002-2006) were constructed for the tidal analysis according to the seasonal groups. Each yearly data series begins on 1st of November of the previous year and ends on 31st of October of the actual year, e.g. the data series year 2002 is: 01.11.2001-31.10. 2002. In each year (2002-2006), the amplitudes of the K1, S2 strain and S1, S2 barometric tidal waves were separately calculated in the D, E and J months by the ETERNA 3.30 program. Averages of the five amplitudes in each group was determined, and presented in Fig. 4. Figure shows clearly that the larger the amplitude of the diurnal barometric wave S1 is the smaller the amplitude of the corresponding strain wave K1. Changes in the semidiurnal band (def_S2 and

bar_S2) are much smaller than in the diurnal band, and changes in the opposite direction are not so pronounced as in the diurnal waves (def_K1 and bar_S1).

3.4. Regression analysis

Regression coefficients were calculated between the strain and atmospheric pressure data series, taking the strain values as a function of the pressure data. Calculation of the regression coefficients was carried out on individual year data and on seasonal segments of the series. Standard deviation of the coefficient's determination varies randomly between 0.1-0.3 nstr/hPa. Results are shown in Fig. 5. In our former publication (Mentes and Eper-Pápai 2006), the phase relationship between deformation and air pressure in tidal frequency bands were investigated, and no phase shift was detected in the Sopronbánfalva Observatory. Regression coefficients were separately calculated for March, April and September, October in the E months' group, and their averages were calculated (E months' average). There is a large difference between coefficients obtained for March, April and September, October. Coefficients of D months and E months' averages differ slightly from the yearly coefficients, especially in 2004-2006. J months' values are smaller than the others, and they reflect the fact that variation of the atmospheric pressure is smallest in summer.

We compared the Fourier amplitude spectra of residual data series after tidal analysis of both corrected and original strain data, to examine whether seasonal correction of strain data yields better results than applying a yearly based linear regression correction. No significant amplitude decrease was found in the diurnal tidal band compared to the one year data processing, which makes the efficiency of seasonal correction questionable. However in the semidiurnal band residual amplitudes decreased by 20-30 % when seasonal groups are applied, and this is 10% improvement against the one year processing. Results from residual inspections agree with Fourier amplitude investigations in Section 3.2 to some extent, as there we found a slight amplitude improvement only in the semidiurnal band.

3.5. Coherence calculations

Coherence analysis was also used to control the efficiency of the regression correction. First we computed coherence between theoretical tide as the input signal, and the uncorrected strain data as the output signal. The coherence function describes the mechanical and electric transmission of our observatory instrument system. Next the computation was repeated using the corrected strain data as the output signal. The results obtained for 2005 are shown in Fig. 6. We obtained similar curves for all of the years we investigated. The coherence value in the semidiurnal band is very nearly 1, in contrast with the diurnal band where it is 0.8 without correction. The suppressed transmission in the diurnal band is in accordance with our former tidal results (Mentes and Eper-Pápai, 2006).

In the diurnal band the efficiency of the correction is somewhat better than in the semidiurnal band. In spite of this fact, the coherence value is smaller than 0.9. It means that either the correction is not effective enough in this frequency band or there are other disturbing effects. Mentes (2002) investigated the effect of temperature variations on deformation data as a possible source of noise, though in that work the long term changes were taken into account without considering tidal frequencies. In the present study we made some comparisons using coherence analysis, taking such data series as output signals, corrected for both pressure and temperature. The resulting coherence values coincide with the barometrically corrected data, and no improvement was found. Our other investigations show that the close phase relationship between temperature and pressure components harden the separation of the different effects.

4. Discussion

Barometric pressure variation and average barometric pressures are smaller in the summer months than in the others (Fig. 1). The situation is the same in the regression coefficients which are also somewhat smaller in J months than in D and E months (Fig. 5). This feature of

the regression coefficients can be more clearly seen in Fig. 7. In this Figure the average regression coefficients, the average amplitudes (determined by tidal analysis) of the barometric waves S1 and S2 obtained for D, E and J months (in 2002-2006) are given for each month. Regression analysis shows that the changes of the regression coefficients along with the variations of the barometric pressure beside a seasonal periodic change also have a random variation.

Spectrum analysis shows the semidiurnal band is less disturbed by barometric pressure variations than the diurnal band. Regression correction also gives better results in the semidiurnal band which is supported by both the spectral amplitude values in Fig. 3 and the residual analysis after tidal calculations. The magnitude of the variations of barometric pressure in the diurnal band is about three times higher than in the semidiurnal band. Monthly amplitude changes of the strain waves are opposite to the amplitude changes of barometric waves in both tidal bands, although it is not obvious at first sight in the semidiurnal band (Figs. 3 and 4). Coherence calculation gives the same results. These findings can be explained by the topography of the observatory. Figure 8 shows the cross section of the surroundings of the observatory constructed from the digital terrain model in the axis of the extensometer. The instrument is perpendicular to the high steep rock face and is about 30 m from it, so the changes of the barometric pressure cause large strain variations in the direction of the extensometer (horizontal arrow in Fig. 8), while the horizontal deformation caused by the vertical pressing force (vertical arrows) can be neglected. The situation is also confirmed by the fact that the tempestuous blasts of wind appear in the extensometric data records, since the steep rock face is perpendicular to the prevailing wind.

The resulting opposite change of the barometric pressure amplitudes relative to the values of the regression coefficients requires explanation which we suppose is in the characteristics of

the topography and properties of the rock (inhomogenities, clefts, faults, etc.) near the observatory. Further investigations are needed to reveal the reasons for this phenomenon.

5. Conclusions

Our investigations brought some new results which aim to improve barometric pressure correction for linear deformation measurements. Seasonally completed regressional correction yields better results than taking a whole year data series. There is about a 10% improvement in the semidiurnal band and no improvement in the diurnal band. However, tidal parameters can be determined with higher accuracy from long continuous data series. Further difficulty arises with seasonal air pressure correction for strain data, since there will be jumps at the turn of the seasons and they should be handled in data processing.

Analysis results show different behaviour of seasonal barometric corrections in the main tidal bands. This raises the need for finite element modelling of our observatory's surroundings to thermal and pressure disturbance investigations.

Acknowledgements

This research was supported by the Hungarian National Scientific Research Fund (OTKA) in the research project K71952. The authors are very grateful to Tibor Molnár for his careful maintenance of the instruments. We thank Walter Zürn and Thomas Jahr for the thorough review of the manuscript which helped to improve this paper.

References

Boy, J-P., Ray, R., Hinderer J., 2006. Diurnal atmospheric tide and induced gravity variations. J. Geodyn. 41, 253-258.

Chapman, S., Lindzen, R.S., 1970. Atmospheric Tides. D. Reidel Publishing Co., Dordrecht, Holland, p. 200.

Dehant, V., 1987. Tidal Parameters for an Unelastic Earth. Physics of the Earth and Planetary Interiors, 49, 97-116.

249 Eper-Pápai, I., Mentes, G., 2002. The Effect of Atmospheric Pressure on Strain
250 Measurements at the Sopron Observatory, Hungary. Bull. d' Inf. Marees Terr. 137, 10901-
251 10906.
252 Farrell, W.E., 1972. Deformation of the Earth Surface Loads. Rev. Geophys. Space Phys. 10
253 (3), 761-797.
254 Kroner, C., Jentzsch, G., 1999. Comparison of Different Barometric Pressure Reductions for
255 Gravity Data and Resulting Consequences. Phys. Earth Planet. Int. 115, 205-218.
256 Kroner, C., Jahr, T., Kuhlmann, S., Fischer, K. D., 2005. Pressure Induced Noise on
257 Horizontal Seismometer and Strainmeter Records Evaluated by Finite Element Modelling.
258 Geophys. J. Int. 161, 167-178, doi:10.1111/j.1365-246X.2005.02576.x.
259 Mentes, G., 1991. Installation of a Quartz Tube Extensometer at the Sopron Observatory.
260 Bull. d'Inf. Marees Terr. 110, 7936-7939.
261 Mentes, G., 2000. Influence of Temperature and Barometric Pressure Variations on
262 Extensometric Deformation Measurements at the Sopron Station. Acta Geod. Geoph. Hung.
263 35 (3), 277-282.
264 Mentes, G., 2004. Atmospheric Tide Obtained by the Microbarograph Developed at the
265 Geodetic and Geophysical Research Institute of the Hungarian Academy of Sciences. Acta
266 Geod. Geoph. Hung. 39 (1), 39-48.
267 Mentes, G., 2005. Results of Tidal Research. Acta Geod. Geoph. Hung. 40 (3-4), 293-305.
268 Mentes, G., 2008. Observation of Recent Tectonic Movements in the Pannonian Basin. J.
269 Geodyn. 45, 169-177.
270 Mentes, G., Eper-Pápai, I., 2006. Investigation of Meteorological Effects on Strain
271 Measurements at Two Stations in Hungary. J. Geodyn. 41 (1-3), 259-267.

Onoue, K., Takemoto, S., 1998. Atmospheric Pressure Effects on Ground Strain Observation at Donzurubo Observatory, Nara, Japan. In: Proceedings of the 13th International Symposium on Earth Tides, Brussels, 22-25 July 1997, 157-164.

Rabbel, W., Zschau, J., 1985. Static Deformations and Gravity Changes at the Earth's Surface due to Atmospheric Loading. J. Geophys. 56, 81-99.

Steffen, H., Kuhlmann, S., Jahr, T., Kroner, C., 2005. Numerical Modelling of the Barometric Pressure Induced Noise in Horizontal Components for the Observatories at Moxa and Schiltach. J. Geodyn. 41, 242-252.

Sun, H.-P., 1995. Static Deformation and Gravity Changes at the Earth' Surface due to the Atmospheric Pressure. PhD Thesis, Cath. Univ. Louvain, Belgium

Van Dam, T.M., Wahr J.M., 1987. Displacements of the Earth's Surface due to Atmospheric Loading: Effects on Gravity and Baseline Measurements. J. Geophys. Res. 92, B2, 1281-1286.

Wahr, J.M., 1981. Body Tides on an Elliptical, Rotating, Elastic and Earth without Oceans. Geophys. J. R. astr. Soc. 64, 677-703.

Wenzel, H.G., 1996. The Nanogal Software: Earth Tide Data Processing Package ETERNA 3.30. Bull. d'Inf. Marees Terr. 124, 9425-9439.

Figure captions

Fig. 1. Average variability of the barometric pressure in different months of 2002-2006 (1 January to 12 December)

Fig. 2. Typical amplitude spectra for measurement data (April 2006)

Fig. 3. Monthly spectrum amplitude differences of strain and theoretical strain (meas.-theor.), corrected strain and theoretical strain (correct.-theor.) as well as amplitudes of barometric waves (barog.) in the diurnal and semidiurnal bands in 2006

Fig. 4. Average of the amplitudes obtained for D, E and J months from 2002 to 2006

Fig. 5. Regression coefficients between barometric and strain data

Fig. 6. Coherence between the theoretical tide and the uncorrected and barometric corrected strain data

Fig. 7. Average regressional coefficients and tidal amplitudes of air pressure data from 2002-2006 for each month

Fig. 8. The cross section of the surroundings of the observatory made from the digital terrain model in the axis of the extensometer. The azimuth of the cross section is 116°.

Figures

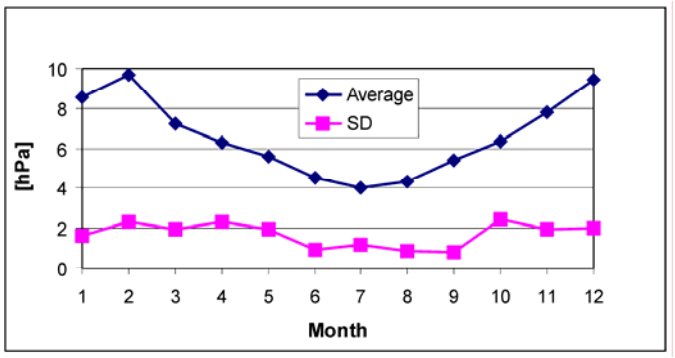

Fig. 1.

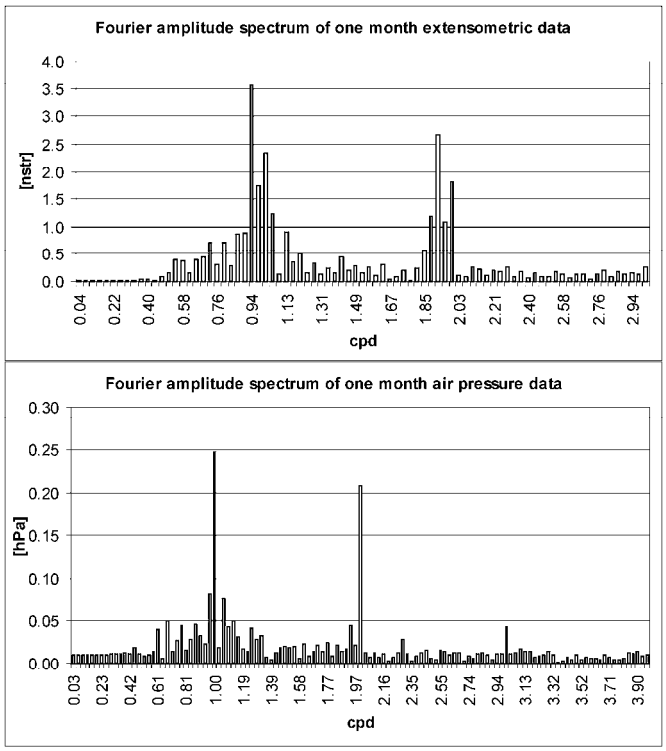

Fig. 2.

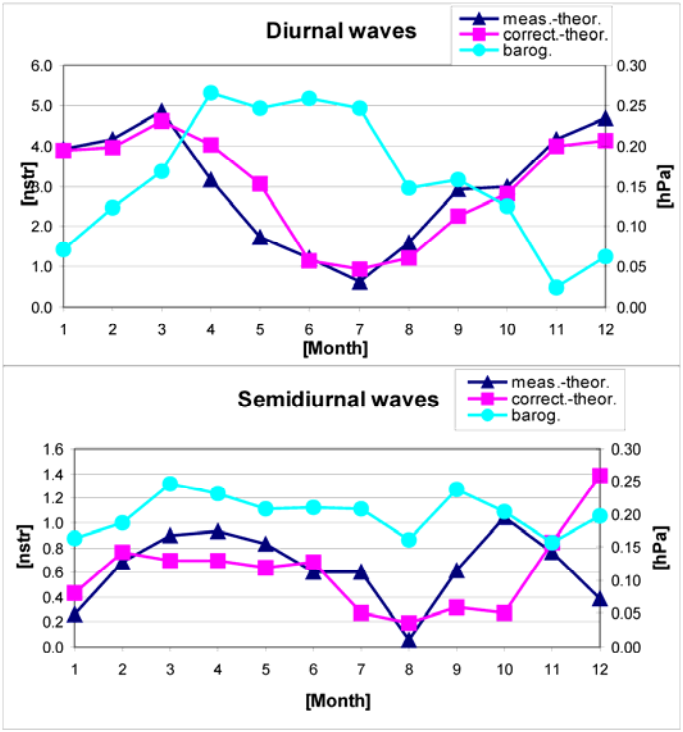

313

314 **Fig. 3.**

315

316

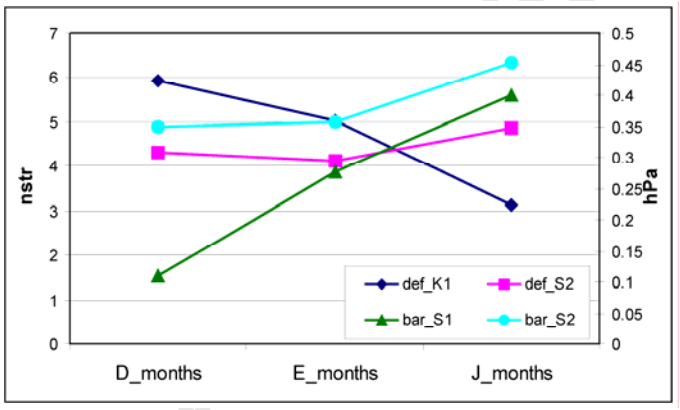

317

318 **Fig. 4.**

319

320

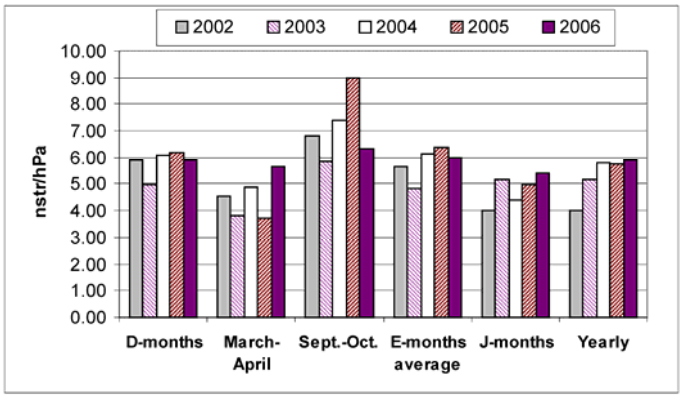

Fig. 5.

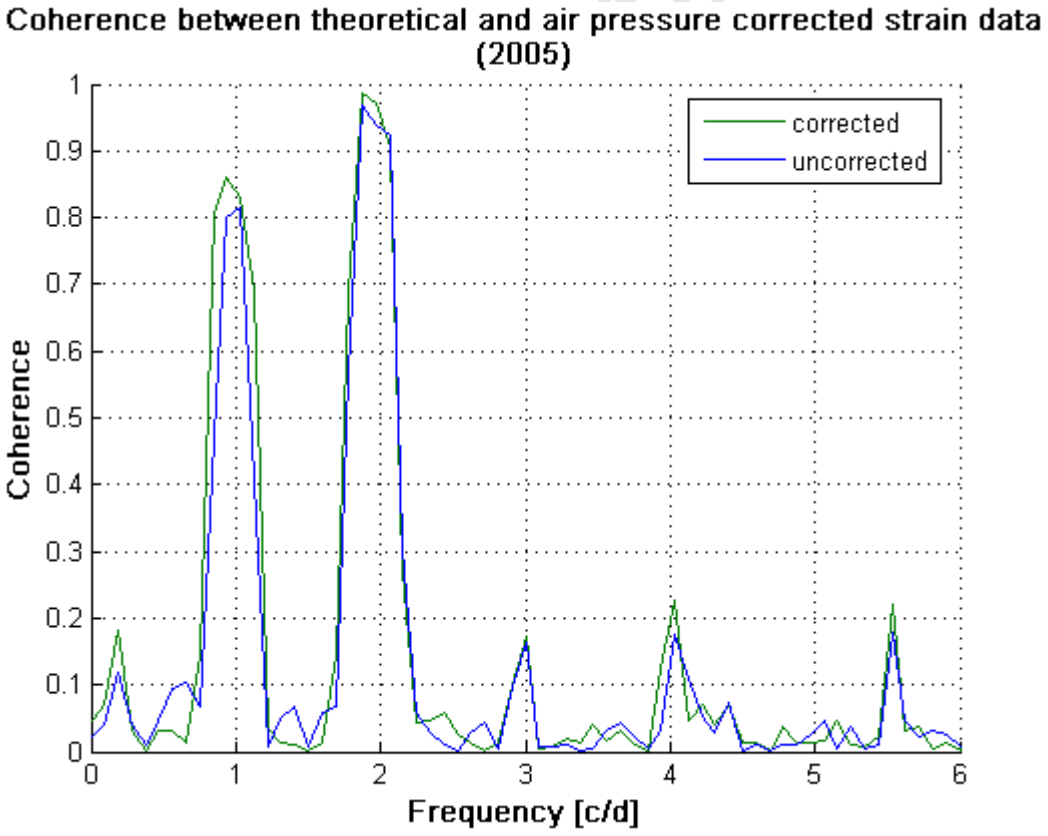

Fig. 6.

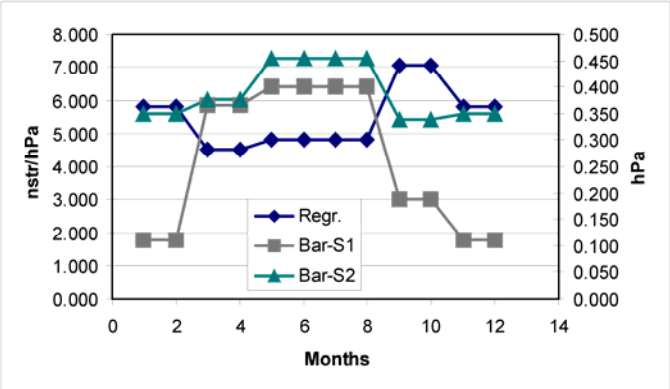

330

331 **Fig. 7.**

332

333

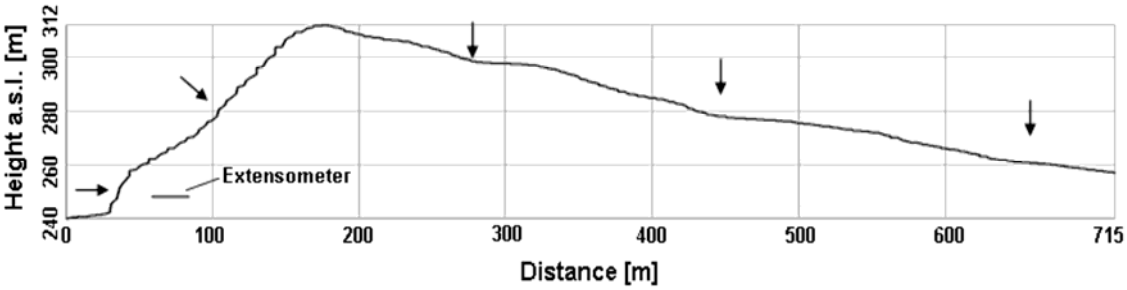

334

335 **Fig. 8.**

336